Abdominal Radiology (2019) 44:2769–2780
https://doi.org/10.1007/s00261-019-02041-z

HEPATOBILIARY

Assessment of liver fibrosis with gadoxetic acid-enhanced MRI: comparisons with transient elastography, ElastPQ, and serologic fibrosis markers

Hyeon Ji Jang[1] · Ji Hye Min[2] · Jeong Eun Lee[1] · Kyung Sook Shin[1] · Kyung-Hee Kim[3] · Seo-Youn Choi[4]

Published online: 30 April 2019

Abstract

Objectives To compare the diagnostic performance of gadoxetic acid-enhanced magnetic resonance imaging (MRI), ultrasonography (US)—based elastography, and serologic fibrosis markers in assessing the stage of liver fibrosis.

Materials and methods This retrospective study included 67 patients (55 male and 12 female; mean age 62.5 years) who underwent gadoxetic acid-enhanced MRI and liver stiffness measurements before liver biopsy or surgery between January 2014 and January 2018. Measurements were performed using transient elastography (TE), ultrasound shear wave elastography point quantification (ElastPQ), and blood tests. The following MRI-based fibrosis markers were assessed: contrast enhancement index (CEI), liver–spleen contrast ratio (LSC), liver–portal vein contrast ratio (LPC), and signal intensity ratio (SIR). The diagnostic performances of fibrosis markers were compared using the area under the receiver operating characteristic curve (AUC), with histopathologic fibrosis stage as the reference standard.

Results The fibrosis stages were F0–F1 ($n=17$), F2 ($n=7$), F3 ($n=20$), and F4 ($n=23$). MRI-based fibrosis markers negatively correlated with histologic stage: CEI ($r=-0.786$); LSC ($r=-0.718$); LPC ($r=-0.448$); and SIR ($r=-0.617$; all $P<0.001$). For diagnosis of either significant liver fibrosis (≥F2) or cirrhosis (F4), the CEI provided better diagnostic accuracy (AUC = 0.898 and 0.881) than the aspartate aminotransferase-to-platelet ratio index (APRI) (AUC = 0.699 and 0.715; all $P<0.05$). The CEI displayed similar diagnostic accuracy for ≥F2 or F4 when using TE (AUC = 0.866 and 0.884, both $P>0.05$) or ElastPQ [AUC = 0.751 ($P=0.021$) and AUC = 0.786 ($P=0.234$)].

Conclusions The CEI measured by gadoxetic acid-enhanced MRI allows the staging of liver fibrosis, with a diagnostic accuracy comparable to that of TE and superior to that of ElastPQ or APRI.

Keywords Gadoxetic acid · Magnetic resonance imaging · Liver cirrhosis · Fibrosis · Elastography

Abbreviations

MRI	Magnetic resonance imaging
TE	Transient elastography
ElastPQ	Ultrasound shear wave elastography point quantification
CEI	Contrast enhancement index
LSC	Liver–spleen contrast ratio
LPC	Liver–portal vein contrast ratio
SIR	Signal intensity ratio

Electronic supplementary material The online version of this article (https://doi.org/10.1007/s00261-019-02041-z) contains supplementary material, which is available to authorized users.

✉ Ji Hye Min
minjh1123@gmail.com

[1] Department of Radiology, Chungnam National University Hospital, Chungnam National University College of Medicine, Daejeon, Republic of Korea

[2] Department of Radiology and Center for Imaging Science, Samsung Medical Center, Sungkyunkwan University School of Medicine, 81 Irwon-Ro Gangnam-gu, Seoul 06351, Republic of Korea

[3] Department of Pathology, Chungnam National University Hospital, Chungnam National University College of Medicine, Daejeon, Republic of Korea

[4] Department of Radiology, Bucheon Hospital, Soonchunhyang University College of Medicine, Bucheon, Republic of Korea

AUC	Area under the receiver operating characteristic curve
APRI	Aspartate aminotransferase-to-platelet ratio index
US	Ultrasound
MRE	Magnetic resonance elastography
AST	Aspartate aminotransferase
SD	Standard deviation
HBP	Hepatobiliary phase
PACS	Picture archiving and communication system
ROI	Region-of-interest
CBD	Common bile duct
SI	Signal intensity
ROC	Receiver operating characteristic

Introduction

Staging of liver fibrosis is important for the clinical management of patients with chronic liver disease because progression of liver fibrosis is associated with a worsening prognosis and an increased risk of developing hepatocellular carcinoma [1, 2]. Liver biopsy is the reference standard for the diagnosis and assessment of liver fibrosis; however, this method is invasive and has limitations, including sampling error, serious complications (e.g., bleeding and infection), and intraobserver and interobserver variability [3–5]. To overcome these issues, several non-invasive methods have been developed for the accurate assessment of liver fibrosis. These methods include the use of blood markers (e.g., aspartate aminotransferase-to-platelet ratio index [APRI]), ultrasound (US) elastography, and magnetic resonance elastography (MRE). In particular, MRE is considered to be the most accurate non-invasive technique for detection and staging of liver fibrosis [6–9]. However, blood markers have limited accuracy in intermediate levels of fibrosis [10], and imaging methods still have problems with reliability, reproducibility, and failure rate [11].

Gadoxetic acid (Eovist or Primovist, Bayer HealthCare, Berlin, Germany) is a liver-specific MR contrast agent that is routinely used for the detection and characterization of liver lesions in clinical practice [12–14]. Both uptake and biliary excretion of gadoxetic acid are related to hepatocyte function, with these processes delayed among cases of liver fibrosis and cirrhosis [15–19]. Several quantitative MRI-based fibrosis markers, such as contrast enhancement index (CEI), liver–spleen contrast ratio (LSC), liver–portal vein contrast ratio (LPC), and signal intensity ratio (SIR) have been reported using the hepatocyte-selective properties of gadoxetic acid [1, 20–23]. However, these methods are not routinely used for the evaluation of fibrosis, due to the lack of validation and comparative studies with other widely accepted elastographic methods.

MRI-based fibrosis markers can easily be measured from gadoxetic acid-enhanced MRI. In addition, most patients scheduled for liver surgery usually also undergo preoperative MRI, so there is no additional burden for patients. Gadoxetic acid-enhanced MRI does not require special equipment for MRE or additional sequences for diffusion-weighted image and perfusion studies.

To our knowledge, there is no report comparing MRI-based fibrosis markers or comparing them with other non-invasive methods, with histopathologic fibrosis stage as the gold standard. We hypothesized that markers of liver fibrosis obtained using gadoxetic acid-enhanced MRI might be robust parameters for assessing the severity of liver fibrosis that are not inferior to other non-invasive methods. Therefore, the purpose of our study was to compare the diagnostic performance of liver fibrosis markers using gadoxetic acid-enhanced MRI, TE, ElastPQ, and the APRI to predict the stage of liver fibrosis.

Materials and methods

This retrospective study was approved by the institutional review board, and the requirement for informed patient consent was waived.

Patients

Between January 2014 and January 2018, a computerized search of patients' medical records identified 137 consecutive patients 18 years or older who underwent gadoxetic acid-enhanced MRI at 3.0 T and who had available pathologic reports of liver fibrosis within 1 month of liver MRI. Among them, we included patients with successful measurement of liver stiffness using TE, ElastPQ (within several days before liver biopsy and surgery), and blood tests (on the same day of liver biopsy or surgery). The exclusion criteria were unavailable TE or ElastPQ measurements ($n=21$); MRI performed with different systems ($n=43$); MRI with severe motion artifacts ($n=3$); and failed measurements using TE or ElastPQ ($n=3$). The final study population comprised of 67 patients (55 male and 12 female; mean age, 62.5 ± 9.5 years, range, 43–85 years) (Fig. 1). The median interval between gadoxetic acid-enhanced MRI and liver biopsy or surgery was 12 days (range 0–30 days).

Blood markers of liver fibrosis

The aspartate aminotransferase-to-platelet ratio index (APRI), a non-invasive serologic fibrosis marker test, was calculated using the formula

$$\mathrm{APRI} = \left(\mathrm{AST}/\mathrm{AST}_{\mathrm{ULN}} * 100\right)/\text{platelet count},$$

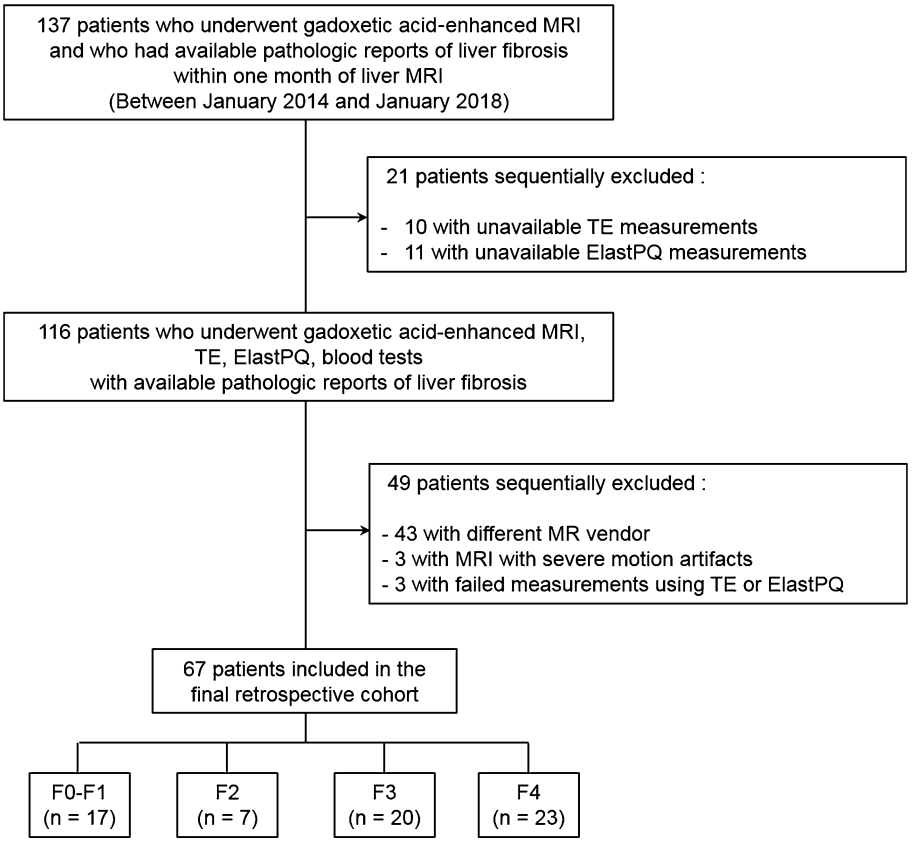

Fig. 1 Flow chart of our study. *MRI* magnetic resonance imaging, *TE* transient elastography, *ElastPQ* ultrasound shear wave elastography point quantification

where AST_{ULN} is the upper limit of the normal AST value (40 IU/L) [24]. Viral hepatitis B infection was diagnosed by the presence of serum hepatitis B surface antigen. Viral hepatitis C infection was diagnosed by the presence of antibodies against hepatitis C virus.

Transient elastography

All patients underwent TE using a FibroScan device (Echosens, Paris, France) by a well-trained technician (with an experience of more than 500 cases of TE), blinded to clinical and histologic data. Liver stiffness measurements were performed in the right lobe of the liver through the intercostal spaces, while each patient was lying supine with the right arm in maximal abduction. The tip of the transducer was placed on the skin between the ribs and aimed at the right lobe of the liver. After the area of measurement (a region 25–65 mm deep) was made, the examiner pressed the probe button to commence data acquisition. A total of ten valid measurements were obtained for each patient. The measurements were expressed in kilopascals, and a success rate of at least 60% was considered reliable. The median value was considered to be representative.

Point shear wave elastography

ElastPQ was performed using an iU-22 ultrasound system (Philips Medical Systems, Bothell, WA, USA) by an abdominal radiologist (J. E. L. with 5 years of ultrasound elastography and 11 years of liver ultrasound experience). The examiner was blinded to all clinical data when the measurements were made. Examinations were performed via an intercostal approach to evaluate the right lobe of the liver, 1–2 cm under the liver capsule, with the patient lying supine with the right arm in maximum abduction. Using real-time B-mode imaging, the examiner positioned the ElastPQ measurement box (approximately 0.5×1.5 cm^2 in size) in a region free of visible ducts or vessels. The patient was instructed to hold their breath while the examiner pressed the ‘‘update’’ button to acquire real-time stiffness measurements. Stiffness is expressed in kilopascals of Young’s modulus. If the amount of non-shear wave motion exceeded the threshold, the system would not calculate the liver stiffness value and displayed only ‘‘0 kPa’’ on the screen. Results < 1 kPa were regarded as invalid measurements. If ten valid measurements could not be obtained after 15 attempts, these cases were considered to be failed measurements. The median value and standard deviation (SD) of 10 valid measurements were obtained and recorded as the liver stiffness values on ElastPQ.

MRI acquisition

MRI was performed using a 3-T MR system (Intera Achieva; Philips Healthcare, Best, the Netherlands) and a 32-channel torso array coil. MRI included the following sequences: in-phase and out-of-phase T1-weighted gradient-recalled-echo imaging; respiratory-triggered two-dimensional fat-suppressed T2-weighted turbo spin-echo imaging; breath-hold fat-suppressed T2-weighted turbo spin-echo imaging; and free-breathing two-dimensional diffusion-weighted imaging with a single-shot echo-planar sequence. Gadoxetic acid-enhanced MRI comprised an unenhanced, arterial phase (20–35 s), a portal phase (60 s), a 3-min transitional phase, and a 20-min hepatobiliary phase (HBP). Gadoxetic acid (Eovist or Primovist, Bayer HealthCare, Berlin, Germany) was administered intravenously at 1–2 mL/s using a power injector (0.025 mmol/kg body weight) for all patients. The bolus injection was followed by a 20 mL saline flush. Details are provided in Supplementary Table 1.

MRI-based fibrosis markers

All images were evaluated using a picture archiving and communication system (PACS) (Maroview V5.4.10.42, INFINITT Healthcare, Seoul, Korea). The region-of-interest (ROI) measurement was applied to the liver parenchyma, muscle, spleen, portal vein, and common bile duct (CBD) of precontrast and/or HBP images (Fig. 2). All ROI measurements were conducted by two radiologists (H. J. J. and J. H. M. with 3 and 11 years of abdominal imaging experience, respectively), independently. The values measured from two radiologists were averaged to minimize measurement error. These radiologists had no knowledge regarding the patients' clinical information.

The signal intensity (SI) of the liver parenchyma was measured in the lateral segment of the left hepatic lobe, segment 4, and the anterior and posterior segments of the right hepatic lobe at the hepatic hilar level on precontrast and HBP images. On the same image, the SIs of the paraspinal muscles on precontrast and HBP images were measured. The SIs of the right and left portal veins, main portal

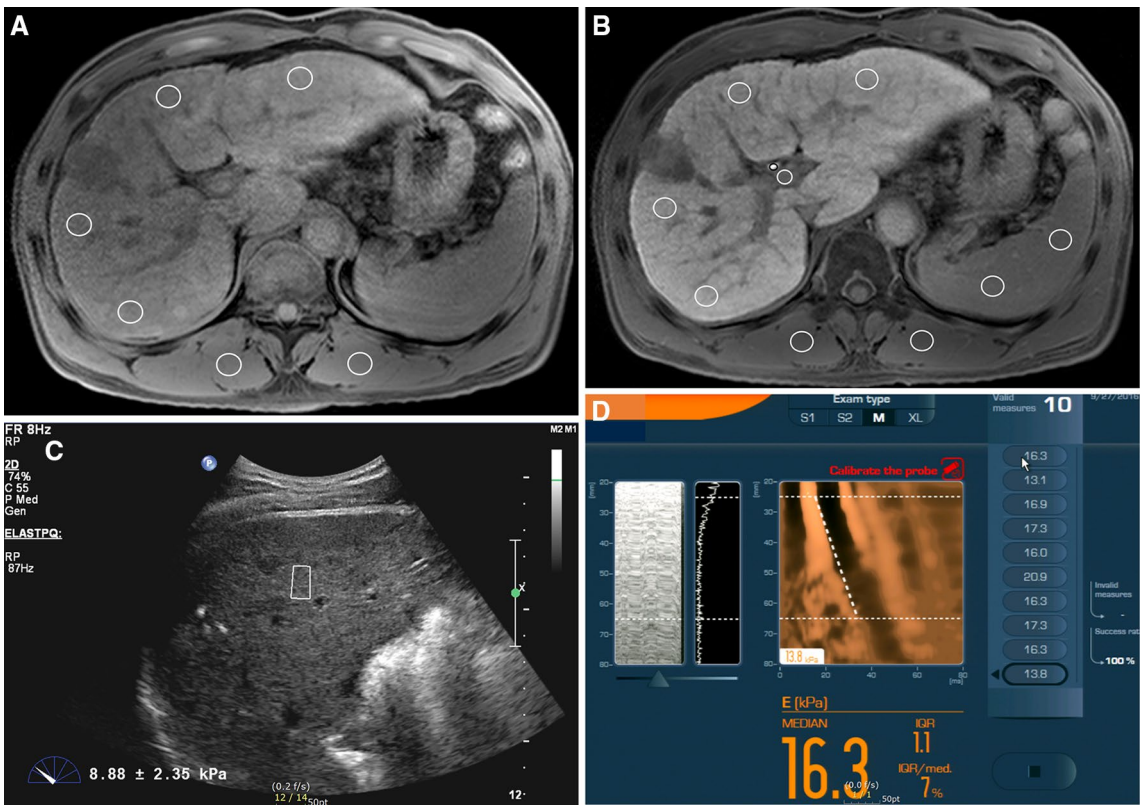

Fig. 2 A 54-year-old man with fibrosis stage F4, and aspartate aminotransferase-to-platelet ratio index 0.78. Circles on the images were region-of-interest (ROI) used for the calculation of MRI-based fibrosis markers on **a** non-contrast image and **b** hepatobiliary phase image of gadoxetic acid-enhanced MRI. The contrast enhancement index value was 1.18. **c** Liver stiffness measurement using ultrasound shear wave elastography point quantification (ElastPQ). The box indicating the ROI was placed in the right lobe of the liver area at a site free of large vessels or visible ducts. The value measured by ElastPQ is shown at the bottom left. **d** Liver stiffness measurement using transient elastography. The median value is shown as 16.3 kPa

vein, common bile duct, and spleen were also measured on HBP images. The SIs of the liver, spleen, and paraspinal muscles were recorded by placing ROIs (approximately 25 mm^2 each) on the three other axial images per section of the liver. Then, the mean value of the four hepatic sections was considered the representative SI of the entire hepatic parenchyma for each phase. Large vessels, bile ducts, focal lesions, and artifacts were carefully avoided when placing ROIs. For the biliary tract and portal vein measurements, the mean SIs were obtained by placing ROIs (4–10 mm^2) over the common bile duct and portal veins. To minimize measurement error from partial volume effects, the portal vein ROIs were located in the center of the portal vein where the portal vein diameter was greater than the slice thickness.

We used four MRI-based fibrosis markers as tentative predictors of liver fibrosis: the liver–spleen contrast ratio (LSC), liver–portal vein contrast ratio (LPC), signal intensity ratio (SIR), and contrast enhancement index (CEI) [1, 20–23, 25]. The LSC corresponded to the ratio of the SI of the liver to that of the spleen as measured on HBP images [25]. The LPC was calculated by dividing the SI of the liver parenchyma by the SI of the portal vein on HBP images [22]. The SIR was calculated as a ratio of the SI of the biliary tract to that of the paraspinal muscles on HBP images [23]. The liver SI ratio was then separately calculated as the ratio of liver to paraspinal muscle SI on non-enhanced images (SIpre) and the ratio of the liver to paraspinal muscle SI on HBP images (SI_{HBP}). The CEI was calculated using the following formula: CEI = [SI_{HBP}]/[SIpre] [20].

Histopathologic analysis

Pathologic examination of the liver was used as the reference standard for liver fibrosis. Sixty-five patients (97.0%) had undergone surgery for hepatic malignancy, and two (3.0%) had undergone percutaneous liver biopsy for an elevated liver function test. All specimens were analyzed by an experienced pathologist (K. H. K. with 16 years of experience) who was blinded to the patients' imaging results and clinical data. The liver fibrosis grade was semiquantitatively evaluated according to the METAVIR scoring system as follows: F0 (no fibrosis); F1 (portal fibrosis without septa); F2 (portal fibrosis with a few septa); F3 (numerous septa without cirrhosis); and F4 (cirrhosis) [26, 27].

Statistical analysis

Continuous variables are expressed as the mean ± standard deviation (SD) with ranges; categorical variables are summarized as counts and percentages. For agreement analysis of the measured SI values and MRI-based fibrosis markers between two observers, the interobserver variability was assessed using the intraclass correlation coefficient across two readers as follows: poor (less than 0.5); moderate (0.5–0.75); good (0.75–0.90); and excellent (0.90–1.00) [28]. Correlations between the results of MRI-based fibrosis markers and histologic staging were analyzed using Spearman correlation coefficients. A correlation was considered to be strong if the absolute value of the correlation coefficient (r) was 0.7–1.0 and moderate if r was 0.4–0.7. The diagnostic performances of the MRI-based fibrosis markers, TE, ElastPQ, and the APRI were evaluated using receiver operating characteristic (ROC) curve analysis, with histopathologic findings as the reference standard. Comparisons of the diagnostic accuracy of the MRI-based fibrosis markers, TE, ElastPQ, and the APRI were estimated by calculating the area under the ROC curve (AUC). All statistical analyses were performed using MedCalc for Windows (MedCalc Software, Mariakerke, Belgium). A P value < 0.05 was considered to indicate statistical significance.

Results

Patient characteristics

The baseline characteristics of the 67 patients are summarized in Table 1. Most of the patients ($n = 54$, 80.6%) had chronic liver disease, of which chronic hepatitis B was the most common etiology ($n = 36$, 53.7%). Histologic stage of liver fibrosis was as follows: F0–F1 ($n = 17$, 25.4%); F2 ($n = 7$, 10.4%); F3 ($n = 20$, 29.9%); and F4 ($n = 23$, 34.3%). The mean liver stiffness values measured using TE and ElastPQ were 12.8 ± 11.8 kPa and 6.3 ± 3.4 kPa, respectively. The mean value of APRI was 1.2 ± 1.6.

Quantitative imaging analysis

Table 2 demonstrates the mean SI values and MRI-based fibrosis markers according to stage of liver fibrosis. The value of MRI-based fibrosis markers decreased as the stage of fibrosis increased ($P < 0.001$). Correlations of the MRI-based fibrosis markers according to the stage of liver fibrosis are illustrated in Fig. 3. All four MRI-based fibrosis markers negatively correlated with fibrotic stage: CEI ($r = -0.786$), LSC ($r = -0.718$), LPC ($r = -0.448$), and SIR ($r = -0.617$; $P < 0.001$ for all comparisons). The intraclass correlation coefficients for measured SI values and MRI-based fibrosis markers across two observers were good or excellent (0.80–0.97). The details of interobserver agreements of the ROI measurements and MRI-based fibrosis markers are in Supplementary Table 2.

Table 1 Demographic and clinical characteristics of the patients ($n=67$)

Characteristic	Value
Age (year)	62.5 ± 9.5 (43–85)
Sex	
Male	55 (82.1)
Female	12 (17.9)
BMI (kg/m^2)	23.4 ± 2.8 (15.8–29.6)
Etiology of chronic liver disease[a]	
Chronic viral hepatitis B	36 (53.7)
Chronic viral hepatitis C	8 (11.9)
Alcoholic liver disease	9 (13.4)
Non-alcoholic fatty liver disease	1 (1.5)
Transient elastography (kPa)	12.8 ± 11.8
ElastPQ (kPa)	6.3 ± 3.4
Blood tests	
Aspartate aminotransferase (IU/L)	54.0 ± 63.9
Alanine aminotransferase (IU/L)	39.3 ± 44.7
Alkaline phosphatase (IU/L)	103.2 ± 63.7
Total bilirubin (mg/dL)	1.0 ± 0.9
Albumin (g/dL)	3.8 ± 0.5
Gamma-glutamyltransferase (IU/L)	161.1 ± 231.5
Platelet count (10^3/mm^3)	168,572.4 ± 75,130.1
APRI	1.2 ± 1.6
Liver fibrosis stage	
F0–F1	17 (25.4)
F2	7 (10.4)
F3	20 (29.9)
F4	23 (34.3)

Continuous variables are described as mean ± standard deviations and range in parentheses and categorical variables are described as number of patients with percentage

BMI body mass index, *ElastPQ* ultrasound shear wave elastography point quantification, *APRI* aspartate aminotransferase-to-platelet ratio index

[a]Among 67 patients, 54 patients (80.6%) had chronic liver disease

Diagnostic performance of MRI-based fibrosis markers

Supplementary Table 3 and Supplementary Fig. 1 show the diagnostic accuracy of the CEI, LSC, LPC, and SIR according to liver fibrosis stage. According to the ROC curve analysis for the diagnosis of significant liver fibrosis (≥ F2) and cirrhosis (F4), the CEI (AUC = 0.898 and 0.881, respectively) tended to show higher AUC values than both the LSC (AUC = 0.847, $P = 0.114$; AUC = 0.874, $P = 0.866$) and SIR (AUC = 0.819, $P = 0.101$; AUC = 0.837, $P = 0.369$). The CEI showed greater diagnostic performance than the LPC (AUC = 0.692, $P = 0.003$; AUC = 0.722, $P = 0.005$).

The CEI showed an AUC of 0.881–0.965 for identifying each stage of liver fibrosis (Table 3). The optimum cutoff value for the diagnosis of significant liver fibrosis (≥ F2) was 1.9 (sensitivity of 84.0% and specificity of 82.4%). For the diagnosis of cirrhosis (F4), the optimum cutoff value was 1.5 (sensitivity of 73.9% and specificity of 88.6%).

Comparisons of the diagnostic performance of MRI-based fibrosis markers with that of TE, ElastPQ, and the APRI

The details of the diagnostic performance of the fibrosis markers are summarized in Tables 3 and 4. Based on the AUCs for the diagnosis of significant liver fibrosis (≥ F2), the CEI had greater diagnostic accuracy (AUC = 0.898) than the APRI (AUC = 0.699, $P = 0.018$) and ElastPQ (AUC = 0.751, $P = 0.021$), and similar diagnostic accuracy to TE (AUC = 0.866, $P = 0.605$). For the diagnosis of cirrhosis (F4), the CEI had greater diagnostic accuracy (AUC = 0.881) than the APRI (AUC = 0.715, $P = 0.027$) and similar diagnostic accuracy to TE (AUC = 0.884, $P = 966$) and ElastPQ (AUC = 0.786, $P = 0.234$). Figure 4 shows the ROC curves of the CEI, TE, ElastPQ, and the APRI for differentiating significant liver fibrosis (≥ F2) and cirrhosis (F4).

Discussion

In our study, we evaluated MRI-based fibrosis markers and compared them with other non-invasive methods, with histopathologic fibrosis stage as the gold standard. All four MRI-based fibrosis markers showed a statistically significant negative correlation with liver fibrosis stage. The CEI was a better marker than LSC, LPC, and SIR for the diagnosis of both significant liver fibrosis (≥ F2) and cirrhosis (F4). Additionally, we found that the CEI derived by gadoxetic acid-enhanced MRI displayed a similar accuracy to that of TE for the diagnosis of significant liver fibrosis (≥ F2) and cirrhosis (F4).

Several studies found that hepatic enhancement with gadoxetic acid is strongly affected by the degree of liver fibrosis [29–32]. Gadoxetic acid is transported from the extracellular space, taken up by hepatocytes via an organic anion transport system, and subsequently secreted into the biliary system [33–38]. Decreases in hepatic enhancement on HBP images suggest that gadoxetic acid uptake by the liver is impaired, whereas the prolongation of hepatic enhancement suggests that gadoxetic acid excretion into bile is also impaired [39–41]. This impaired gadoxetic acid uptake by the liver may be caused by a decrease in the number of normal hepatocytes or a decrease in gadoxetic acid uptake by hepatocytes, and impaired gadoxetic acid excretion may be caused by hepatocyte dysfunction [40].

In advanced liver fibrosis, the CEI is reduced owing to a decreased number of normal hepatocytes (caused by fibrotic

Table 2 Signal intensity and MRI-based fibrosis markers according to the stage of liver fibrosis

	F0–F1 ($n=17$)	F2 ($n=7$)	F3 ($n=20$)	F4 ($n=23$)	*P* value
SI on precontrast images					
Liver	902.3 ± 187.9	885.8 ± 129.0	1004.0 ± 154.3	1033.7 ± 195.2	0.010
Paraspinal muscles	1063.8 ± 225.1	981.0 ± 205.8	947.0 ± 198.9	1004.2 ± 207.7	0.340
SI on HBP image					
Liver	1018.0 ± 161.6	972.9 ± 213.9	838.8 ± 210.0	961.8 ± 238.3	0.261
Paraspinal muscles	495.1 ± 85.1	488.4 ± 131.0	502.9 ± 147.1	691.0 ± 225.0	0.001
Spleen	530.3 ± 100.4	523.3 ± 118.4	556.4 ± 180.7	797.8 ± 343.4	0.001
Portal vein	701.6 ± 191.8	606.6 ± 151.7	644.5 ± 186.1	855.2 ± 387.7	0.089
CBD	1903.2 ± 238.9	1641.9 ± 442.7	1539.8 ± 297.8	1530.0 ± 443.8	0.001
MRI-based fibrosis markers					
CEI	2.3 ± 0.5	2.3 ± 0.3	1.6 ± 0.2	1.4 ± 0.2	< 0.001
LSC	2.0 ± 0.4	1.9 ± 0.3	1.6 ± 0.3	1.3 ± 0.3	< 0.001
LPC	1.5 ± 0.3	1.6 ± 0.3	1.3 ± 0.2	1.2 ± 0.2	< 0.001
SIR	3.9 ± 0.6	3.4 ± 0.7	3.3 ± 1.0	2.4 ± 0.8	< 0.001

Values are expressed as means ± standard deviations

SI signal intensity, HBP hepatobiliary phase; *CBD* common bile duct, *CEI* contrast enhancement index, *LSC* liver–spleen contrast ratio, *LPC* liver–portal vein contrast ratio, *SIR* signal intensity ratio

tissue growth) or a reduction in gadoxetic acid uptake owing to severe hepatocyte dysfunction, degeneration, or necrosis [41]. In agreement with our results, Watanabe et al. reported that the CEI is significantly more correlated with liver fibrosis stage than other variables, such as hepatocyte necrosis and reduced cell function [41]. Lee et al. reported that the CEI was constantly and significantly decreased with increasing severity of cirrhosis [20], which was consistent with the current results. However, in the previous study, liver cirrhosis was clinically diagnosed, and the severity of cirrhosis was not grouped by liver biopsy findings [20]. A strong point of our study is that we used histopathologic specimens as a reference standard rather than clinical staging systems.

In addition to the CEI, several other MRI-based fibrosis markers have been used for staging liver fibrosis. The LSC (a widely accepted method) and LPC (as a substitute for the LSC) are simple assessments of relative hepatic enhancement using the spleen or portal vein as representatives of the blood pool [18, 25, 42–44]. These markers are focused on the plasma and extracellular extravascular space exposed to blood contrast agent concentrations [43]. Therefore, they may not reflect liver fibrosis directly, but instead may be correlated with liver function parameters [22, 25]. In addition, Noda et al. reported that the SIRs of cystic duct and common bile duct on gadoxetic acid-enhanced MRI correlated with Child–Pugh score, MELD score, and APRI [23]. In our study, SIR has a negative correlation with the fibrosis stage, but is less reliable than CEI. In addition, it may be difficult to accurately assess the degree of liver fibrosis with the SIR, which utilizes reduced biliary tract contrast enhancement during the HBP in patients with hepatic dysfunction.

In our study, the CEI had better diagnostic accuracy than the APRI, and similar diagnostic accuracy to TE and ElastPQ, for the diagnosis of significant liver fibrosis (≥ F2) and cirrhosis (= F4). The APRI is the simplest, most widely used non-invasive method for estimating the stage of liver fibrosis among patients with chronic viral hepatitis C [45, 46]. However, Yilmaz et al. [47] reported that the reliability of the APRI was insufficient for staging liver fibrosis among patients with chronic viral hepatitis B, as their serum AST levels fluctuate owing to disease flares. TE was one of the earliest investigated methods for measuring liver stiffness, offering high accuracy and precision for assessing the stage of liver fibrosis [48, 49]. However, TE and ElastPQ are limited in their diagnostic capabilities owing to failure rates, reliability issues, interobserver and intraobserver variability, and reproducibility across US elastography systems [11]. Given that the SI values on gadoxetic acid-enhanced MRI can be reliably measured with excellent interobserver agreement and are significantly correlated with liver fibrosis stage, the CEI might be a useful alternative imaging biomarker for the evaluation of liver fibrosis.

Our study has some limitations. First, the retrospective design could have led to selection bias. Our study cohort had mixed etiologies of chronic liver disease, most of which were chronic hepatitis B infection. Further studies assessing diagnostic performances and reliability of MRI-based fibrosis markers in non-viral liver diseases should be performed. Second, the sample size was rather small. Third, multiple variables are involved in liver disease. The underlying cause of cirrhosis may influence the degree of hepatic enhancement because liver cirrhosis of varying

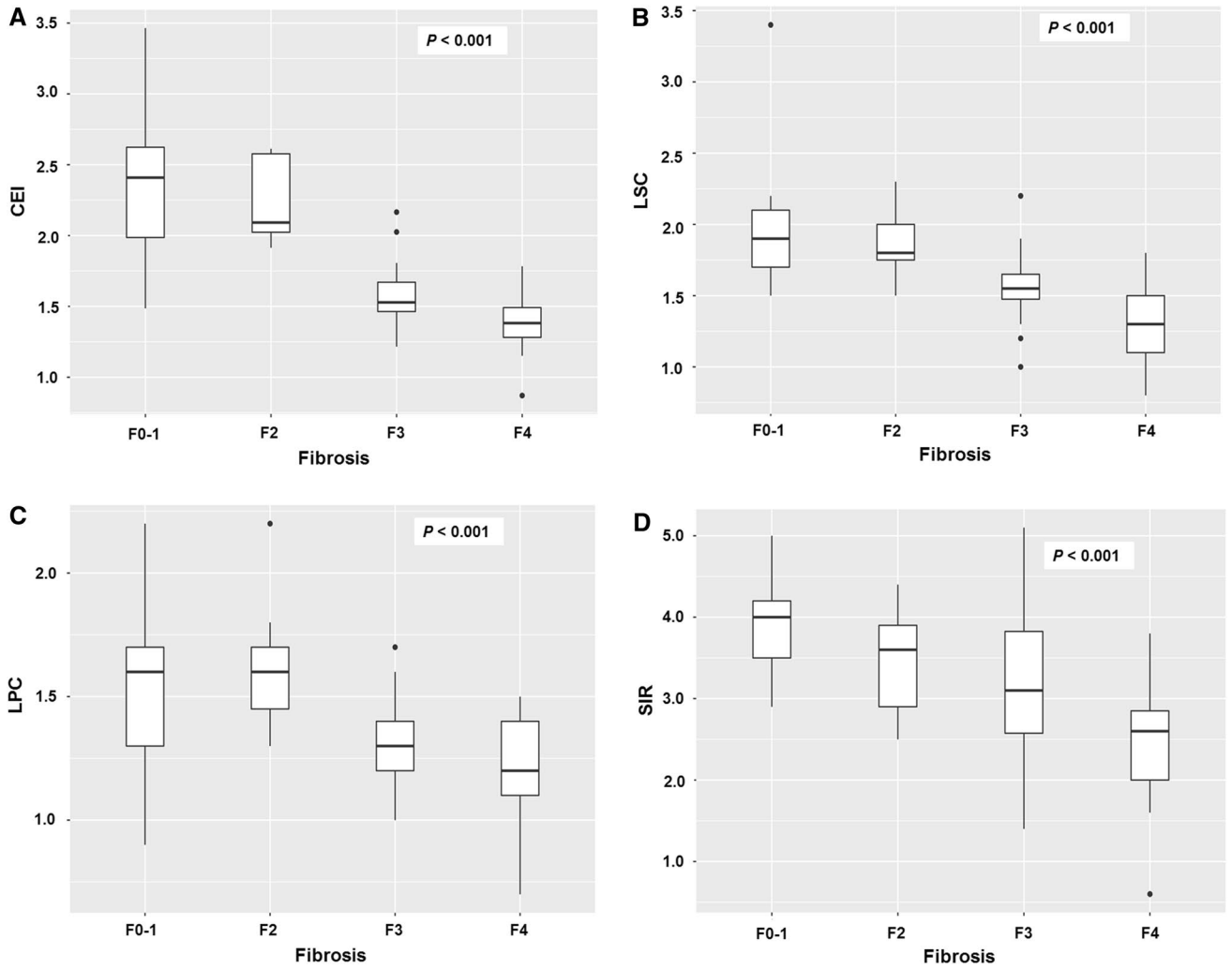

Fig. 3 Boxplots of the liver stiffness values according to the stage of liver fibrosis. **a** Contrast enhancement index (CEI). **b** Liver–spleen contrast ratio (LSC). **c** Liver–portal vein contrast ratio (LPC). **d** Signal intensity ratio (SIR). The boxes represent the interquartile ranges, with the thick lines within the boxes representing the median values. The error bars indicate the smallest and largest values within 1.5 box lengths of the 25th and 75th percentiles, respectively. The dots are outliers representing very large values that deviate markedly from the range of observed data

causes is associated with different pathologic cirrhosis patterns. Fourth, because our study was performed on 3.0-T MRI from a single manufacturer, it may limit the ability to generalize our results. Fifth, the CEI does not include consideration of tissues within the portal circulation, and thus, variations in portal pressure may have affected our results. Sixth, we were unable to compare the performance of our MRI-based fibrosis markers to that of MR elastography for staging liver fibrosis. Finally, we did not perform a validation study using another group of patients.

In conclusion, our results showed that the CEI measured by gadoxetic acid-enhanced MRI is an accurate fibrosis marker for staging liver fibrosis, with a diagnostic accuracy comparable to that of TE. The CEI may be a potential imaging-based fibrosis marker that does not place any additional burden on the patient.

Funding We declare no sources of financial support or funding received from any organization including National Institutes of Health (NIH); Wellcome Trust; Howard Hughes Medical Institute (HHMI).

Compliance with ethical standards

Conflict of interest All author declares that they have no conflict of interest.

Ethical approval All procedures performed in studies involving human participants were in accordance with the ethical standards of the insti-

Table 3 Diagnostic performance of the fibrosis markers according to the stage of liver fibrosis (F1–F4)

Parameter	≥F1	≥F2	≥F3	F4
CEI				
AUC	0.892 (0.793–0.955)	0.898 (0.799–0.958)	0.965 (0.889–0.995)	0.881 (0.779–0.948)
Cutoff [criterion]	2.0	1.9	1.8	1.5
Sensitivity (%)	87.3 (75.5–94.7)	84.0 (70.9–92.8)	95.4 (84.2–99.4)	73.9 (51.6–89.8)
Specificity (%)	83.3 (51.6–97.9)	82.4 (56.6–96.2)	91.7 (73.0–99.0)	88.6 (75.4–96.2)
P value	< 0.001	< 0.001	< 0.001	< 0.001
TE				
AUC	0.884 (0.782–0.949)	0.866 (0.761–0.937)	0.906 (0.810–0.964)	0.884 (0.782–0.949)
Cutoff [criterion]	7.5	7.7	7.7	10.3
Sensitivity (%)	72.7 (59.0–83.9)	76.0 (61.8–86.9)	86.1 (72.1–94.7)	82.6 (61.2–95.0)
Specificity (%)	83.3 (51.6–97.9)	94.1 (71.3–99.9)	91.7 (73.0–99.0)	84.1 (69.9–93.4)
P value	< 0.001	< 0.001	< 0.001	< 0.001
ElastPQ				
AUC	0.742 (0.621–0.842)	0.751 (0.630–0.848)	0.794 (0.678–0.883)	0.786 (0.668–0.876)
Cutoff [criterion]	4.04	4.89	4.89	5.34
Sensitivity (%)	72.7 (59.0–83.9)	68.0 (53.3–80.5)	76.7 (61.4–88.2)	87.0 (66.4–97.2)
Specificity (%)	66.7 (34.9–90.1)	82.4 (56.6–96.2)	88.3 (62.6–95.3)	72.7 (57.2–85.0)
P value	< 0.001	< 0.001	< 0.001	< 0.001
APRI				
AUC	0.765 (0.646–0.860)	0.699 (0.575–0.805)	0.656 (0.529–0.767)	0.715 (0.591–0.819)
Cutoff [criterion]	0.31	0.31	0.44	0.44
Sensitivity (%)	76.4 (63.0–86.8)	78.0 (64.0–88.5)	62.8 (46.7–77.0)	87.0 (66.4–97.2)
Specificity (%)	66.7 (34.9–90.1)	58.8 (32.9–81.6)	66.7 (44.7–84.4)	61.4 (45.5–75.6)
P value	0.001	0.010	0.034	0.002

Values in parentheses are 95% confidence interval

CEI contrast enhancement index, *AUC* area under the receiver operating characteristic curve, *TE* transient elastography, *ElastPQ* ultrasound shear wave elastography point quantification, *APRI* aspartate aminotransferase-to-platelet ratio index

Table 4 Comparison of diagnostic performance of the fibrosis markers according to the stage of liver fibrosis (F1–F4)

Marker	≥F1	≥F2	≥F3	F4
CEI	0.892 (0.793–0.955)	0.898 (0.799–0.958)	0.965 (0.889–0.995)	0.881 (0.779–0.948)
TE	0.884 (0.782–0.949)	0.866 (0.761–0.937)	0.906 (0.810–0.964)	0.884 (0.782–0.949)
ElastPQ	0.742 (0.621–0.842)	0.751 (0.630–0.848)	0.794 (0.678–0.883)	0.786 (0.668–0.876)
APRI	0.765 (0.646–0.860)	0.699 (0.575–0.805)	0.656 (0.529–0.767)	0.715 (0.591–0.819)
P value (CEI versus TE)	0.884	0.605	0.218	0.966
P value (CEI versus ElastPQ)	0.016	0.021	0.003	0.234
P value (CEI versus APRI)	0.167	0.018	< 0.001	0.027

Values in parentheses are 95% confidence interval

CEI contrast enhancement index, *TE* transient elastography, *ElastPQ* ultrasound shear wave elastography point quantification, *APRI* aspartate aminotransferase-to-platelet ratio index

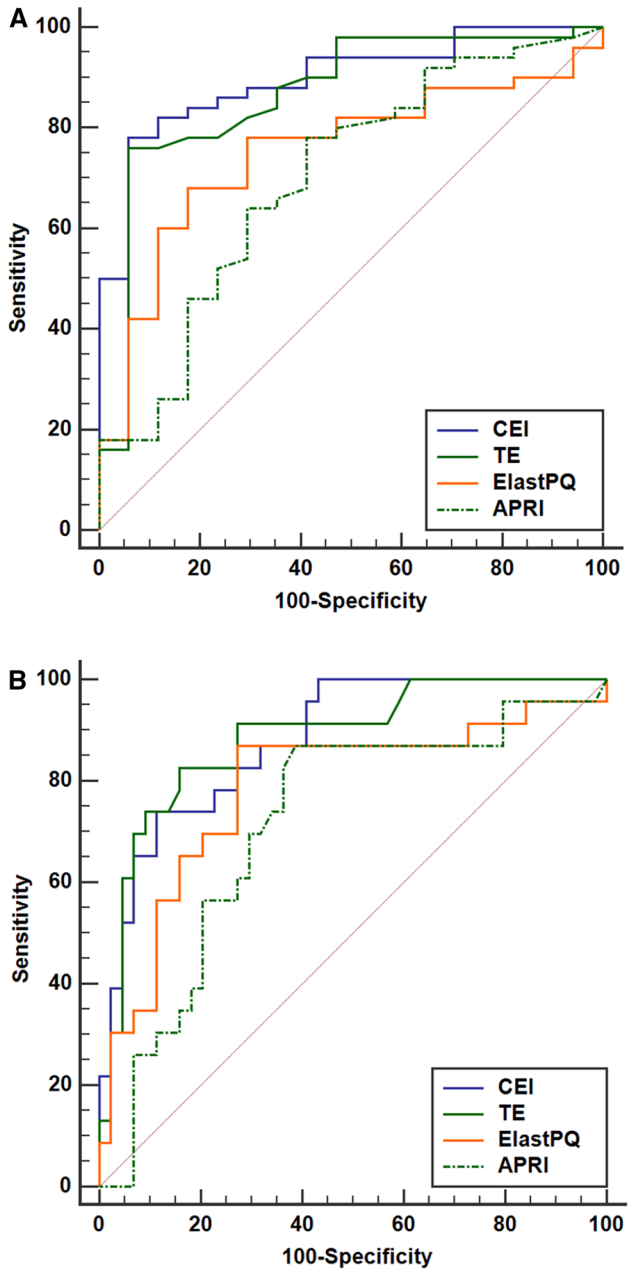

Fig. 4 Receiver operating characteristic curves of MRI-based fibrosis markers for differentiating **a** significant liver fibrosis and **b** cirrhosis. Values were based on the liver stiffness or scores measured with the contrast enhancement index (CEI), transient elastography (TE), ultrasound shear wave elastography point quantification (ElastPQ), and aspartate aminotransferase-to-platelet ratio index (APRI)

tutional and/or national research committee and with the 1964 Helsinki Declaration and its later amendments or comparable ethical standards. Informed consent was waived for retrospective nature of clinical and imaging data collection in this study.

References

1. Motosugi U, Ichikawa T, Oguri M, Sano K, Sou H, Muhi A, Matsuda M, Fujii H, Enomoto N, Araki T (2011) Staging liver fibrosis by using liver-enhancement ratio of gadoxetic acid-enhanced MR imaging: comparison with aspartate aminotransferase-to-platelet ratio index. Magn Reson Imaging 29:1047-1052. https://doi.org/10.1016/j.mri.2011.05.007
2. Yoshida H, Shiratori Y, Moriyama M, Arakawa Y, Ide T, Sata M, Inoue O, Yano M, Tanaka M, Fujiyama S, Nishiguchi S, Kuroki T, Imazeki F, Yokosuka O, Kinoyama S, Yamada G, Omata M (1999) Interferon therapy reduces the risk for hepatocellular carcinoma: national surveillance program of cirrhotic and noncirrhotic patients with chronic hepatitis C in Japan. IHIT Study Group. Inhibition of Hepatocarcinogenesis by Interferon Therapy. Ann Intern Med 131:174-181
3. Regev A, Berho M, Jeffers LJ, Milikowski C, Molina EG, Pyrsopoulos NT, Feng ZZ, Reddy KR, Schiff ER (2002) Sampling error and intraobserver variation in liver biopsy in patients with chronic HCV infection. Am J Gastroenterol 97:2614-2618. https://doi.org/10.1111/j.1572-0241.2002.06038.x
4. Bedossa P, Carrat F (2009) Liver biopsy: the best, not the gold standard. J Hepatol 50:1-3. https://doi.org/10.1016/j.jhep.2008.10.014
5. Rockey DC, Caldwell SH, Goodman ZD, Nelson RC, Smith AD (2009) Liver biopsy. Hepatology 49:1017-1044. https://doi.org/10.1002/hep.22742
6. Horowitz JM, Venkatesh SK, Ehman RL, Jhaveri K, Kamath P, Ohliger MA, Samir AE, Silva AC, Taouli B, Torbenson MS, Wells ML, Yeh B, Miller FH (2017) Evaluation of hepatic fibrosis: a review from the society of abdominal radiology disease focus panel. Abdom Radiol (NY) 42:2037-2053. https://doi.org/10.1007/s00261-017-1211-7
7. Singh S, Venkatesh SK, Wang Z, Miller FH, Motosugi U, Low RN, Hassanein T, Asbach P, Godfrey EM, Yin M, Chen J, Keaveny AP, Bridges M, Bohte A, Murad MH, Lomas DJ, Talwalkar JA, Ehman RL (2015) Diagnostic performance of magnetic resonance elastography in staging liver fibrosis: a systematic review and meta-analysis of individual participant data. Clin Gastroenterol Hepatol 13:440-451.e446. https://doi.org/10.1016/j.cgh.2014.09.046
8. Venkatesh SK, Yin M, Ehman RL (2013) Magnetic resonance elastography of liver: technique, analysis, and clinical applications. J Magn Reson Imaging 37:544-555. https://doi.org/10.1002/jmri.23731
9. Venkatesh SK, Ehman RL (2015) Magnetic resonance elastography of abdomen. Abdom Imaging 40:745–759. https://doi.org/10.1007/s00261-014-0315-6
10. Rockey DC, Bissell DM (2006) Noninvasive measures of liver fibrosis. Hepatology 43:S113–120. https://doi.org/10.1002/hep.21046
11. Kennedy P, Wagner M, Castera L, Hong CW, Johnson CL, Sirlin CB, Taouli B (2018) Quantitative Elastography Methods in Liver Disease: Current Evidence and Future Directions. Radiology 286:738-763. https://doi.org/10.1148/radiol.2018170601
12. Asayama Y, Tajima T, Nishie A, Ishigami K, Kakihara D, Nakayama T, Okamoto D, Fujita N, Aishima S, Shirabe K, Honda H (2011) Uptake of Gd-EOB-DTPA by hepatocellular carcinoma: radiologic-pathologic correlation with special reference to bile production. Eur J Radiol 80:e243-248. https://doi.org/10.1016/j.ejrad.2010.10.032
13. Kobayashi S, Matsui O, Gabata T, Koda W, Minami T, Ryu Y, Kozaka K, Kitao A (2012) Relationship between signal intensity on hepatobiliary phase of gadolinium ethoxybenzyl diethylenetriaminepentaacetic acid (Gd-EOB-DTPA)-enhanced MR imaging

and prognosis of borderline lesions of hepatocellular carcinoma. Eur J Radiol 81:3002-3009. https://doi.org/10.1016/j.ejrad.2012.03.029
14. Akai H, Matsuda I, Kiryu S, Tajima T, Takao H, Watanabe Y, Imamura H, Kokudo N, Akahane M, Ohtomo K (2012) Fate of hypointense lesions on Gd-EOB-DTPA-enhanced magnetic resonance imaging. Eur J Radiol 81:2973-2977. https://doi.org/10.1016/j.ejrad.2012.01.007
15. Verloh N, Haimerl M, Rennert J, Muller-Wille R, Niessen C, Kirchner G, Scherer MN, Schreyer AG, Stroszczynski C, Fellner C, Wiggermann P (2013) Impact of liver cirrhosis on liver enhancement at Gd-EOB-DTPA enhanced MRI at 3 Tesla. Eur J Radiol 82:1710-1715. https://doi.org/10.1016/j.ejrad.2013.05.033
16. Ryeom HK, Kim SH, Kim JY, Kim HJ, Lee JM, Chang YM, Kim YS, Kang DS (2004) Quantitative evaluation of liver function with MRI Using Gd-EOB-DTPA. Korean J Radiol 5:231-239. https://doi.org/10.3348/kjr.2004.5.4.231
17. Tamada T, Ito K, Higaki A, Yoshida K, Kanki A, Sato T, Higashi H, Sone T (2011) Gd-EOB-DTPA-enhanced MR imaging: evaluation of hepatic enhancement effects in normal and cirrhotic livers. Eur J Radiol 80:e311-316. https://doi.org/10.1016/j.ejrad.2011.01.020
18. Nishie A, Asayama Y, Ishigami K, Tajima T, Kakihara D, Nakayama T, Takayama Y, Okamoto D, Taketomi A, Shirabe K, Fujita N, Obara M, Yoshimitsu K, Honda H (2012) MR prediction of liver fibrosis using a liver-specific contrast agent: Superparamagnetic iron oxide versus Gd-EOB-DTPA. J Magn Reson Imaging 36:664-671. https://doi.org/10.1002/jmri.23691
19. Tsuda N, Okada M, Murakami T (2010) New proposal for the staging of nonalcoholic steatohepatitis: evaluation of liver fibrosis on Gd-EOB-DTPA-enhanced MRI. Eur J Radiol 73:137-142. https://doi.org/10.1016/j.ejrad.2008.09.036
20. Lee S, Choi D, Jeong WK (2016) Hepatic enhancement of Gd-EOB-DTPA-enhanced 3 Tesla MR imaging: Assessing severity of liver cirrhosis. J Magn Reson Imaging 44:1339-1345. https://doi.org/10.1002/jmri.25288
21. Goshima S, Kanematsu M, Watanabe H, Kondo H, Kawada H, Moriyama N, Bae KT (2012) Gd-EOB-DTPA-enhanced MR imaging: prediction of hepatic fibrosis stages using liver contrast enhancement index and liver-to-spleen volumetric ratio. J Magn Reson Imaging 36:1148-1153. https://doi.org/10.1002/jmri.23758
22. Zhang W, Wang X, Miao Y, Hu C, Zhao W (2018) Liver function correlates with liver-to-portal vein contrast ratio during the hepatobiliary phase with Gd-EOB-DTPA-enhanced MR at 3 Tesla. Abdom Radiol (NY) 43:2262-2269. https://doi.org/10.1007/s00261-018-1462-y
23. Noda Y, Goshima S, Kajita K, Kawada H, Kawai N, Koyasu H, Matsuo M, Bae KT (2016) Biliary tract enhancement in gadoxetic acid-enhanced MRI correlates with liver function biomarkers. Eur J Radiol 85:2001-2007. https://doi.org/10.1016/j.ejrad.2016.09.003
24. Lin ZH, Xin YN, Dong QJ, Wang Q, Jiang XJ, Zhan SH, Sun Y, Xuan SY (2011) Performance of the aspartate aminotransferase-to-platelet ratio index for the staging of hepatitis C-related fibrosis: an updated meta-analysis. Hepatology 53:726-736. https://doi.org/10.1002/hep.24105
25. Motosugi U, Ichikawa T, Sou H, Sano K, Tominaga L, Kitamura T, Araki T (2009) Liver parenchymal enhancement of hepatocyte-phase images in Gd-EOB-DTPA-enhanced MR imaging: which biological markers of the liver function affect the enhancement? J Magn Reson Imaging 30:1042-1046. https://doi.org/10.1002/jmri.21956
26. Bedossa P, Poynard T (1996) An algorithm for the grading of activity in chronic hepatitis C. The METAVIR Cooperative Study Group. Hepatology 24:289-293. https://doi.org/10.1002/hep.510240201
27. Group FMCS (1994) Intraobserver and interobserver variations in liver biopsy interpretation in patients with chronic hepatitis C. The French METAVIR Cooperative Study Group. Hepatology 20:15-20
28. Koo TK, Li MY (2016) A Guideline of Selecting and Reporting Intraclass Correlation Coefficients for Reliability Research. J Chiropr Med 15:155-163. https://doi.org/10.1016/j.jcm.2016.02.012
29. Verloh N, Utpatel K, Haimerl M, Zeman F, Fellner C, Fichtner-Feigl S, Teufel A, Stroszczynski C, Evert M, Wiggermann P (2015) Liver fibrosis and Gd-EOB-DTPA-enhanced MRI: A histopathologic correlation. Sci Rep 5:15408. https://doi.org/10.1038/srep15408
30. Choi YR, Lee JM, Yoon JH, Han JK, Choi BI (2013) Comparison of magnetic resonance elastography and gadoxetate disodium-enhanced magnetic resonance imaging for the evaluation of hepatic fibrosis. Invest Radiol 48:607-613. https://doi.org/10.1097/RLI.0b013e318289ff8f
31. Feier D, Balassy C, Bastati N, Stift J, Badea R, Ba-Ssalamah A (2013) Liver fibrosis: histopathologic and biochemical influences on diagnostic efficacy of hepatobiliary contrast-enhanced MR imaging in staging. Radiology 269:460-468. https://doi.org/10.1148/radiol.13122482
32. Noren B, Forsgren MF, Dahlqvist Leinhard O, Dahlstrom N, Kihlberg J, Romu T, Kechagias S, Almer S, Smedby O, Lundberg P (2013) Separation of advanced from mild hepatic fibrosis by quantification of the hepatobiliary uptake of Gd-EOB-DTPA. Eur Radiol 23:174-181. https://doi.org/10.1007/s00330-012-2583-2
33. Pascolo L, Cupelli F, Anelli PL, Lorusso V, Visigalli M, Uggeri F, Tiribelli C (1999) Molecular mechanisms for the hepatic uptake of magnetic resonance imaging contrast agents. Biochem Biophys Res Commun 257:746-752. https://doi.org/10.1006/bbrc.1999.0454
34. Tsuboyama T, Onishi H, Kim T, Akita H, Hori M, Tatsumi M, Nakamoto A, Nagano H, Matsuura N, Wakasa K, Tomoda K (2010) Hepatocellular carcinoma: hepatocyte-selective enhancement at gadoxetic acid-enhanced MR imaging--correlation with expression of sinusoidal and canalicular transporters and bile accumulation. Radiology 255:824-833. https://doi.org/10.1148/radiol.10091557
35. Tsuda N, Matsui O (2010) Cirrhotic rat liver: reference to transporter activity and morphologic changes in bile canaliculi--gadoxetic acid-enhanced MR imaging. Radiology 256:767-773. https://doi.org/10.1148/radiol.10092065
36. van Montfoort JE, Stieger B, Meijer DK, Weinmann HJ, Meier PJ, Fattinger KE (1999) Hepatic uptake of the magnetic resonance imaging contrast agent gadoxetate by the organic anion transporting polypeptide Oatp1. J Pharmacol Exp Ther 290:153-157
37. Weinmann HJ, Bauer H, Frenzel T, Muhler A, Ebert W (1996) Mechanism of hepatic uptake of gadoxetate disodium. Acad Radiol 3 Suppl 2:S232-234
38. Lee NK, Kim S, Kim GH, Heo J, Seo HI, Kim TU, Kang DH (2012) Significance of the "delayed hyperintense portal vein sign" in the hepatobiliary phase MRI obtained with Gd-EOB-DTPA. J Magn Reson Imaging 36:678-685. https://doi.org/10.1002/jmri.23700
39. Ni Y, Marchal G, Lukito G, Yu J, Muhler A, Baert AL (1994) MR imaging evaluation of liver enhancement by Gd-EOB-DTPA in selective and total bile duct obstruction in rats: correlation with serologic, microcholangiographic, and histologic findings. Radiology 190:753-758. https://doi.org/10.1148/radiology.190.3.8115623
40. Kim T, Murakami T, Hasuike Y, Gotoh M, Kato N, Takahashi M, Miyazawa T, Narumi Y, Monden M, Nakamura H (1997) Experimental hepatic dysfunction: evaluation by MRI with Gd-EOB-DTPA. J Magn Reson Imaging 7:683-688

41. Watanabe H, Kanematsu M, Goshima S, Kondo H, Onozuka M, Moriyama N, Bae KT (2011) Staging hepatic fibrosis: comparison of gadoxetate disodium-enhanced and diffusion-weighted MR imaging--preliminary observations. Radiology 259:142-150. https://doi.org/10.1148/radiol.10100621
42. Takatsu Y, Kobayashi S, Miyati T, Shiozaki T (2016) A novel method for evaluating enhancement using gadolinium-ethoxybenzyl-diethylenetriamine penta-acetic acid in the hepatobiliary phase of magnetic resonance imaging. Clin Imaging 40:1112-1117. https://doi.org/10.1016/j.clinimag.2016.07.001
43. Dahlqvist Leinhard O, Dahlstrom N, Kihlberg J, Sandstrom P, Brismar TB, Smedby O, Lundberg P (2012) Quantifying differences in hepatic uptake of the liver specific contrast agents Gd-EOB-DTPA and Gd-BOPTA: a pilot study. Eur Radiol 22:642-653. https://doi.org/10.1007/s00330-011-2302-4
44. Esterson YB, Flusberg M, Oh S, Mazzariol F, Rozenblit AM, Chernyak V (2015) Improved parenchymal liver enhancement with extended delay on Gd-EOB-DTPA-enhanced MRI in patients with parenchymal liver disease: associated clinical and imaging factors. Clin Radiol 70:723-729. https://doi.org/10.1016/j.crad.2015.03.005
45. Lu Q, Lu C, Li J, Ling W, Qi X, He D, Liu J, Wen T, Wu H, Zhu H, Luo Y (2016) Stiffness Value and Serum Biomarkers in Liver Fibrosis Staging: Study in Large Surgical Specimens in Patients with Chronic Hepatitis B. Radiology 280:290-299. https://doi.org/10.1148/radiol.2016151229
46. Shaheen AA, Myers RP (2007) Diagnostic accuracy of the aspartate aminotransferase-to-platelet ratio index for the prediction of hepatitis C-related fibrosis: a systematic review. Hepatology 46:912-921. https://doi.org/10.1002/hep.21835
47. Yilmaz Y, Yonal O, Kurt R, Bayrak M, Aktas B, Ozdogan O (2011) Noninvasive assessment of liver fibrosis with the aspartate transaminase to platelet ratio index (APRI): Usefulness in patients with chronic liver disease: APRI in chronic liver disease. Hepat Mon 11:103-106
48. Barr RG, Ferraioli G, Palmeri ML, Goodman ZD, Garcia-Tsao G, Rubin J, Garra B, Myers RP, Wilson SR, Rubens D, Levine D (2015) Elastography Assessment of Liver Fibrosis: Society of Radiologists in Ultrasound Consensus Conference Statement. Radiology 276:845-861. https://doi.org/10.1148/radiol.2015150619
49. Friedrich-Rust M, Ong MF, Martens S, Sarrazin C, Bojunga J, Zeuzem S, Herrmann E (2008) Performance of transient elastography for the staging of liver fibrosis: a meta-analysis. Gastroenterology 134:960-974. https://doi.org/10.1053/j.gastro.2008.01.034